RESEARCH ARTICLE

Macromolecular Bioscience
www.mbs-journal.de

Ultrasensitive and Selective Impedimetric Determination of Prostate Specific Membrane Antigen Based on Di-Succinimide Functionalized Polythiophene Covered Cost-Effective Indium Tin Oxide

Elif Burcu Aydın, Muhammet Aydın, and Mustafa Kemal Sezgintürk*

A new and ultrasensitive impedimetric biosensor fabricated by using conjugated di-succinimide substituted polythiophene (P(ThidiSuc)) polymer modified indium tin oxide electrode is developed for the first time to detect the prostate specific membrane antigen (PSMA). The polymer P(Thi-diSuc) is synthesized by using a simple way and used in the fabrication of the proposed biosensor. The synthesized polymer contains di-succinimide groups, which offers covalent immobilization of PSMA specific antibodies. The developed strategy shortens the biosensor fabrication steps, because these active groups bind covalently to the amino ends of PSMA specific antibodies and this reaction does not require any crosslinking agent. Various characterization studies like impedimetric and voltammetric measurements, and morphological analyses are utilized to confirm the successful development of the biosensor. Under optimum conditions, the biosensing ability of the PSMA determination has a wide linear determination range from 0.015 to 14.4 pg mL^{-1}, as well as a low limit of detection of 6.4 fg mL^{-1} and a high sensitivity of 1.36 kohm pg^{-1} mL cm^{-2}. Furthermore, the proposed biosensor is able to measure the PSMA antigen in real human serums, which offers that it is a simple, low-cost, and sensitive tool with excellent potential for application in the quantification of PSMA.

1. Introduction

Prostate cancer is the most prevalent type of cancer disease and it causes death to almost 12% of all cancer cases.[1,2] For early diagnosis of prostate cancer, measurement of the blood concentration of prostate specific antigen (PSA) and digital rectal exam are the usually utilized prostate cancer diagnosis methods.[2,3] Nevertheless, the main obstruction of PSA analysis is its low specificity that causes a high negative biopsy rate. Furthermore, PSA is not a specific marker of prostate cancer because with some conditions such as benign prostatic hyperplasia and non-specific inflammation the PSA level is high.[4–8] Thus, a specific, more-sensitive and more-effective biomarkers is necessary for prostate cancer diagnosis with new cancer biomarker like Prostate specific membrane antigen (PSMA).[9,10]

PSMA (folate hydrolase I and glutamate carboxypeptidase II) is a type II transmembrane zinc-metalloenzyme with glutamate carboxypeptidase activity.[11] It catalyzes the hydrolysis reaction of *N*-acetyl aspartyl glutamate to glutamate and it is synthesized at high concentrations in prostate cancer cells.[2,12] Furthermore, it is synthesized at low concentrations in benign prostatic epithelium.[12] The concentrations of PSMA in prostate cell is associated to the aggressiveness of tumor growth.[13] Serum PSMA levels are found as 600 and 50 ng mL^{-1} in prostate cancer patients and healthy individuals, respectively.[13] In addition, PSMA is also a tumor marker for diagnosis of prostate cancer in urine and seminal fluid. In the case of prostate cancer, the PSMA level is increased from 25 to 350 ng mL^{-1} in urine.[14] Mhawech-Fauceglia et al. (2007) reported that though PSMA is produced in other malignancies, it is known as a quite sensitive and specific biomarker of prostate cancer. Therefore, PSMA detection can offer a valuable alternative for the diagnosis of prostate cancer.[15] For the quantitative detection of PSMA, Western blot or enzyme-linked immunosorbent assay (ELISA) are usually utilized and they possess some drawbacks such as having long and time-consuming procedure, matrix interference, and high cost.[16] Electrochemical detection methods offer rapid, direct, and sensitive detection of target analytes such as cancer biomarkers in complicated samples.[17–20] Electrochemical biosensors are major types of biosensors owing to their superiorities such as small size, portability, lower cost than other kinds of biosensors.[21,22] The portability and small dimension provide electrochemical

E. B. Aydın, M. Aydın
Scientific and Technological Research Center
Tekirdağ Namık Kemal University
Tekirdağ 59100, Turkey
E-mail: ebbahadir@nku.edu.tr
Prof. M. K. Sezgintürk
Faculty of Engineering, Bioengineering Department
Çanakkale Onsekiz Mart University
Çanakkale 17020, Turkey

The ORCID identification number(s) for the author(s) of this article can be found under https://doi.org/10.1002/mabi.202100173

DOI: 10.1002/mabi.202100173

biosensors to be utilized as a point-of-care tool by the patients at their home or in the hospital. Because of this, they are a proper tool for PSMA biosensing applications.[1,23]

A versatile love wave sensor based on molecularly imprinted polymer (MIP) was developed for PSMA determination. PSMA was a template and simple reversible addition/fragmentation chain transfer precipitation polymerization was employed to enhance the specific template binding. The real-time resonance frequency was used to determine the PSMA levels and the frequency increased with the PSMA level in the linear range of 0.01–100 ng mL^{-1}. The detection limit of this system was 0.013 ng mL^{-1}.[9] A different approach based on micromechanical pillars was used for determination of PSMA. Anti-PSMA antibody functionalized pillars was used for PSMA detection and the linear detection range of this system was 0.3–100 nM.[24] An optically transparent patterned ITO combined with a microfluidic channel was fabricated for impedimetric biosensing of PSMA. In this system, gold nanoparticles (AuNPs) modified anti-PSMA antibody provided the specificity of this system. In addition, AuNPs improved the electron transfer features and increased the PSMA antibody loading efficiency, thus a high sensitivity was obtained. The dynamic range and detection limit were obtained as 19–6250 and 12.5 ng mL^{-1}, respectively.[12] A different nanosensor for PSMA detection was developed by using Fe_3O_4@Ag magnetic nanocomposite modified artificial antibody composed of low-molecular-weight PSMA synthetic inhibitor. This composite allowed an easy magnetic isolation of PSMA employing external magnetic force and PSMA was detected via magnetically assisted surface enhanced Raman spectroscopy. The detection limit of this system was 6 pM. This method had a good repeatability and the Fe_3O_4@anti-PSMA@Ag composite was stable for 21 days.[2]

Electrochemical impedance spectroscopy (EIS) is an attractive technique for investigation on the electrode surface variations through the sinusoidal electric potential application with a variable frequency. EIS measures antibody-antigen biointeractions as electrical signals directly and does not require a labeling procedure and a pretreatment step. This easy and fast detection increased the applicability feature of this system.[25–28] EIS investigates the resistance and capacitance that occur on the electrode surface that displays the biological immobilization processes. This property makes EIS appropriate for measurement of antibody-antigen interactions[29–32]

Conjugated polymers are promising materials used for the fabrication of electrochemical biosensors. They have taken considerable interest on account of their unique features such as good electrical conductivity, lower costs, great biocompatibility, and good stability. Therefore, they have been employed in several areas such as chemical sensors/biosensors development, medical analysis, and drug delivery applications.[33,34] They are known as a suitable material for attachment of biological molecules and they provide fast electron transfer during the biosensor development.[35,36] The characterization of polyheterocycles, such as polypyrrole, polythiophene, polyaniline, and poly(3,4-ethylenedioxythiophene) were performed in the 1980s. Among these polymers, polythiophene is one of the most extensively used π-conjugated polymers.[37] They have used in many applications because some of them integrate suitable processability and high stability with an ability to detect, transduce, and amplify different physical and chemical data into an electrical or optical response. The possibility of modifying the structure to change some physical features is the primary advantage of polythiophene polymers.[38]

In this paper, we describe an impedimetric immunosensor using *P(Thi-diSuc)* modified ITO substrate for highly sensitive detection of PSMA biomarker. Anti-PSMA antibody was utilized as a molecular recognition molecule and covalently attached on the ITO surface through the usages of a thin polymer layer. EIS, cyclic voltammetry (CV), atomic force (AFM), and scanning electron microscopy (SEM) measurements were performed to support the success of the immunosensor construction steps. The SEM and AFM images of the *P(Thi-diSuc)* polymer coated ITO confirmed the dense, complete, and homogenous morphology of polymer. The uniformity of polymer layer offered anti-PSMA antibodies to be immobilized to the functional succinimide groups of *P(Thi-diSuc)* polymer in a uniform and homogenous manner, which provided great importance with regard to the sensitivity and the reproducibility of immunosensors. The developed immunosensor had a simple surface modification process and the molecular recognition element was easily anchored on the ITO surface without using any crosslinking agent. During the biosensor fabrication, both the concentration of *P(Thi-diSuc)* and anti-PSMA antibodies, and the incubation durations were optimized and evaluated. The electrochemical responses caused with the different concentrations of PSMA antigen were recorded. The results displayed an excellent correlation between the PSMA antigen concentration and EIS signal. Furthermore, the suggested biosensor was able to quantify the PSMA antigen in human serum samples. The proposed immunosensor offered a simple and low-cost aspect to determine PSMA antigen and provided a new surface matrix that suggested an excellent sensing capability.

2. Experimental Section

The materials, reagents, and apparatus used in this study are given in the Supporting Information file.

2.1. Synthesis Procedures of Immobilization Matrix Material

2.1.1. Synthesis Procedure of Di-Succinimide Groups Functionalized Thiophene Monomer (Thi-diSuc)

The twins succinimide groups functionalized thiophene monomer was synthesized from simple esterification reaction between one equivalent 3-thiophenemalonic acid and two equivalents of *N*-hydroxy succinimide at 35 °C under an argon gas by modifying the processes found in literature.[33,34] The 4-dimethylamino pyridine (0.224 g, 2 mmol, 0.2 equiv.) and 1-(3-dimethylaminopropyl)-3-ethylcarbodiimide hydrochloride (7.64 g, 40 mmol, 4 equiv.) were solved in 50 mL dry tetrahydrofuran at room temperature under argon gas. The 3-thiophenemalonic acid (1.86 g, 10 mmol, 1 equiv.) and *N*-hydroxy succinimide (2.30 g, 20 mmol, 2 equiv.) were added to this solution, and it was stirred at room temperature for 2 days. And then, it was filtered and evaporated to dryness under vacuum. The remaining solid mixture was dissolved in dichloromethane and after that, it was extracted with brine solution (saturated

NaCl solution) and ultrapure water (50 mL) four times. Finally, the organic layer was dried, filtrated, and solvent was evaporated. The final product was obtained by column chromatography (hexane/ethyl acetate) 5:1, v/v) (2.28 g, 60%, yield). FTIR(ATR) cm^{-1}: 3098; 2957-2926(CH); 1820(C═O); 1780(C═O); 1715(C═O);1365; 1194; 1043; 885; 881; 790; 724; 642. (Figure S2B, Supporting Information). Raman (λ_{laser} = 780 nm): 2970, 2948 (CH); 1811, 1780 (C═O); 1730 (C═O); 1410; 1150; 1058; 946; 882; 832; 760; 668 (Figure S3B, Supporting Information). ^{1}H-NMR (δH, ppm) (400 MHz, $CDCl_3$): 7.33 ppm (Ha, 1H), 7.08 ppm (Hb, 1H), 7.26 ppm (Hc, 1H), 3.97 ppm (Hd, 1H), and 2.80 ppm (He, 8H) (Figure S4, Supporting Information). Ha/Hb/Hc/Hd/He-(1H)/(1H)/(1H)/(1H)/(8H) (1/1/1/1/8).

2.1.2. Synthesis Procedure of Di-Succinimide Group Functionalized Polythiophene Polymer P(Thi-diSuc)

The *P(Thi-diSuc)* polymer was generated by using chemical oxidation polymerization technique with minor adaptations using ferric chloride.[34,39] A solution of anhydrous ferric chloride (1.94 g, 12 mmol) in 11.5 mL of CH_3NO_2 was added dropwise over 20 min to a solution of (1.14 g, 3.0 mmol) of monomer in 35 mL of CCl_4 at 0 °C. The mixture was stirred at room temperature under a flux of argon gas for 120 min. The molar ratio of the oxidant to monomer was 4:1. The polymer suspension was precipitated in a large excess of methanol (400 mL). The polymer was collected by filtration, purified by repeated rinsing with fresh methanol (using a Soxhlet apparatus) and with ultrapure water to remove the residual $FeCl_3$ and the oligomers to yield the pure polymer. The polymer was dried under vacuum at 40 °C overnight (0.46 g, 41%, yield). FTIR (ATR, cm^{-1}): 2962, 2921-2850(C–H); 1814, 1780, 1731 (C═0); 1420; 1367; 1258; 1202; 1065; 796; 645 (Figure S2C, Supporting Information). Raman (λ_{laser} = 780 nm): 1820, 1770, 1735 (C═O); 1444; 1162; 1063; 940; 857; 714; 645 (Figure S3C, Supporting Information).

2.2. Preparation of *P(Thi-diSuc)* Covered ITO Electrode and Biomolecule Immobilization

Prior to modification, the ITO was cleaned by successive sonication in acetone, soap solution and ultra-pure water for 10 min and then, dried under an argon stream. The stepwise fabrication is represented in **Scheme 1**. The synthesized P(Thi-diSuc) polymer (0.26 mg mL^{-1}) was solved in acetone and 30 µL polymer solution was dropped onto the clean ITO electrode surface. After that, the spin-coater was accelerated to 1000 rpm rotational speed for 60 s and then dried under reduced pressure at room temperature. The active carboxyl ends of *P(Thi-diSuc)* polymer linked to the amino group of anti-PSMA antibodies through covalent bond. The obtained *P(Thi-diSuc)* modified ITO was immersed in anti-PSMA solution for 45 min and subsequently, rinsed with ultrapure water to eliminate physically adsorbed antibodies and dried under an argon stream. Afterwards, the free succinimide ends of the polymer were obstructed by BSA to prevent nonspecific adsorption event. Subsequently, the ITO/*P(Thi-diSuc)*/anti-PSMA/BSA electrode was washed with ultra-pure water and dried by using an argon stream. The resulting modified electrode was ready to analyze PSMA antigen concentration and stored at 4 °C for further use.

2.3. Electrochemical Analysis of PSMA Antigen

For analysis of PSMA antigen, ITO/*P(Thi-diSuc)*/anti-PSMA/BSA bioelectrode was incubated in 50 mM phosphate buffered saline (PBS) (pH 7.4) including PSMA antigen for 30 min followed by washing with water and then, transferred to the electrochemical cell with 5 mM $[Fe(CN)_6]^{3-/4-}$ and 1 M KCl solution. The EIS frequency range, alternating potential and formal potential were 0.5 Hz–50 kHz, 5 mV, and 0 V, respectively. The CV scan range and scan rate were found as −0.5–1.0 V and 100 mV s^{-1}, respectively.

2.4. Interference Study

EIS analyses of the ITO/*P(Thi-diSuc)*/anti-PSMA/BSA bioelectrode incubated with interference biomarkers in the absence and presence of PSMA in 5 mM $[Fe(CN)_6]^{3-/4-}$ 1 M KCl were studied. KLK4, IL 8, IL 6, and IL 1α were utilized as interference biomarkers and before incubation they were added in PBS solution. Afterwards, the EIS of the ITO/*P(Thi-diSuc)*/anti-PSMA/BSA bioelectrode was recorded.

2.5. Detection of PSMA Antigen in Real Human Serum

The human serums were provided from Tekirdağ Namık Kemal University, Faculty of Medicine (2013/86/07/05 with ethic committee approval number). The samples were further diluted with PBS (50 mM, pH 7.4) 1000-fold. Afterwards, ITO/*P(Thi-diSuc)*/anti-PSMA/BSA electrodes were utilized to measure PSMA antigen in human serums. To analyze the accuracy of the proposed biosensor standard addition technique was performed.

3. Results and Discussion

Herein, we reported an ultrasensitive PSMA immunosensor prepared by using conjugated di-succinimide substituted polythiophene polymer. First of all, due to commendable price of ITO, it was chosen as transducer for biosensing system development. Moreover, ITO had prominent electrochemical and physical characteristics. The characteristics consisted in this biosensor fabrication procedure containing: 1) conjugated *P(Thi-diSuc)* polymer, which was selected as the immobilization matrix for biorecognition molecules because of its favorable microenvironment, high biocompatibility, good stability, and good electron transfer ability; 2) succinimide groups of polymer, which could bind directly to amino ends of anti-PSMA antibodies; and 3) successful attachment of PSMA specific antibody on the ITO substrate, which provided selective platform for PSMA antigen immobilization. The combination of the above advantages resulted in excellent sensitivity, good selectivity, and high stability for detection of PSMA antigen.

The entire ITO electrode modification is briefly described in Scheme 1. The biosensor preparation process consisted of four

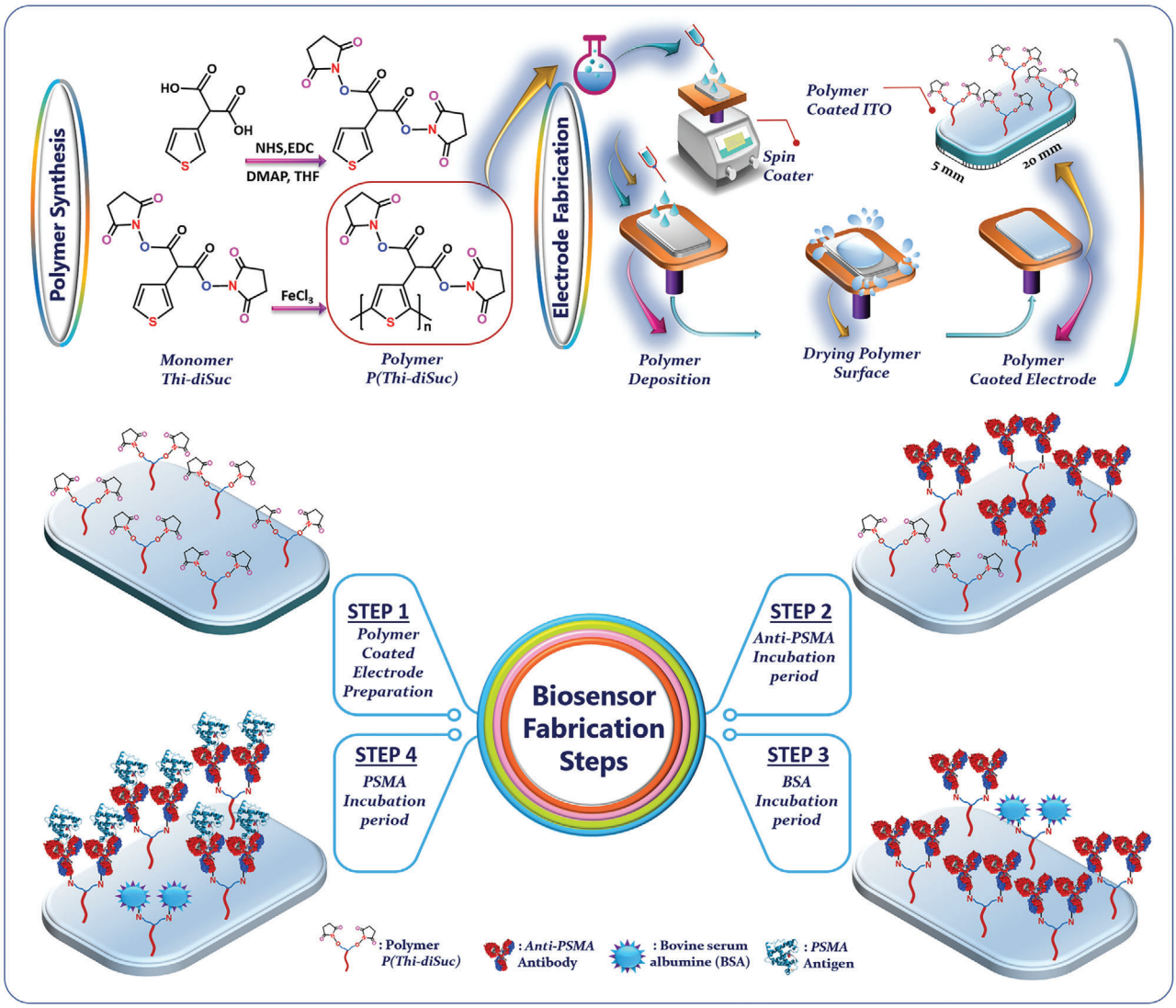

Scheme 1. Polymer *P(Thi-diSuc)* synthesis and step-by-step fabrication of the suggested biosensor.

steps. First, the ITO surface was modified with *P(Thi-diSuc)* polymer to generate succinimide groups on the electrode surface. Since polymer molecules were uniformly dispersed on the electrode surface, they not only formed succinimide groups on the ITO platform for biomolecule immobilization but also, they enlarged the surface area (Step 1). The anti-PSMA biorecognition molecules were covalently attached on the electrode surface via strong amide bond formation between polymer and antibody (Step 2). Subsequently, BSA molecules were immobilized on the free succinimide ends to block nonspecific interactions (Step 3). Finally, the target analyte (PSMA antigen) was detected electrochemically.

In this work, the thiophene structure was selected as main backbone for interface material which possessed unique advantages (soluble, simple processability, and environmental stability). In the monomer design, two succinimide groups was fixed on thiophene malonic acid, because NHS ester terminal groups are best candidate for using to covalently couple amino including biological molecules (e.g., proteins, peptides, enzymes, and antibodies) to surfaces via amide bonds. For monomer (*Thi-diSuc*), the used strategy consisted of synthesizing the ester bond between thiophene malonic acid and *N*-hydroxysuccinimide through Steglich esterification reaction that was one of the proper ways for the production of ester groups. For polymer *P(Thi-diSuc)* synthesis, the oxidative coupling polymerization reaction strategy, which had unique benefits (e.g., soluble and simple processability) was used. The synthetic procedures of the thiophene monomer and the corresponding polymers are depicted in Scheme 1. The as-prepared monomer and polymer were fully examined by FTIR, RAMAN, and ^{1}H NMR spectroscopies, which is consistent with their expected molecular structures. The details for their characterization results are provided in Supporting Information file.

The chemical composition and surface features of the polymer covered ITO sheet and anti-PSMA bound ITO surface were characterized via FTIR and Raman spectroscopy (**Figure 1**). The FTIR

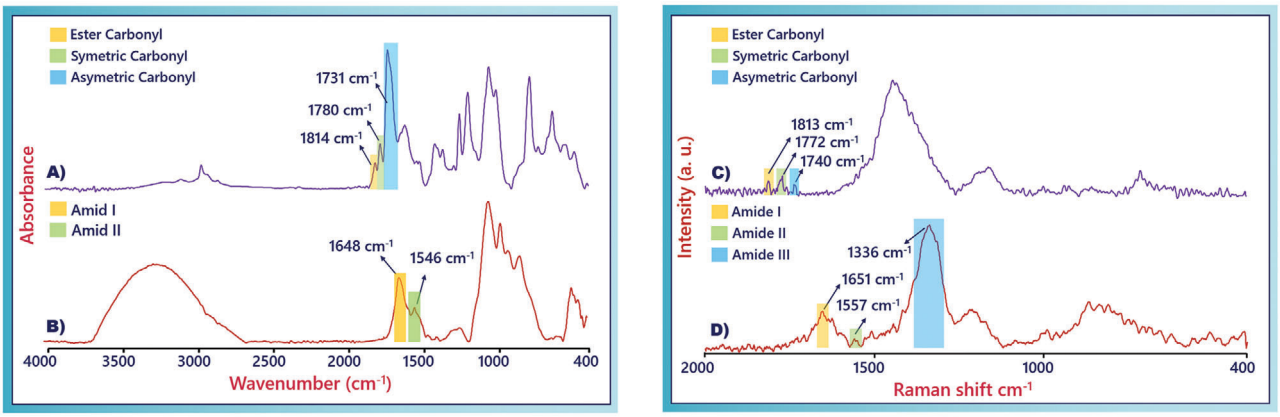

Figure 1. FTIR A,B) and Raman C,D) spectra of before and after anti-PSMA binding.

spectra of *P(Thi-diSuc)* polymer (A) and anti-PSMA (B) modified ITO surfaces are demonstrated in Figure 1, respectively. As illustrated in Figure 1A, the most characteristic peaks of succinimide groups are symmetric carbonyl stretch at 1780 cm^{-1} (broader), asymmetric carbonyl stretch at 1731 cm^{-1} (much stronger).[40,41] And also bands at lower energy (symmetric ν(C–N–C) stretch of succinimide groups and asymmetric ν(C–N–C) stretch of succinimide groups) were seen at 1367 and 1202 cm^{-1}, respectively which were known as additional succinimidyl group identifiers.[41] The peak at 1065 cm^{-1} was attributed to ν(C–N–C) stretch of succinimide groups. The medium peak at 1814 cm^{-1} was the conformation of the typical carbonyl stretching vibration of as-formed new ester bond.[33,34] These findings confirmed the presence of the polymer interface material on ITO surface. The FTIR spectroscopy is a widely employed technology for the analyses of biocomponent samples. As shown in Figure 1B, the strong evidence of aminolysis reactions between NHS groups of *P(Thi-diSuc)* and amino groups of antibodies were the disappearance of symmetric and asymmetric bands and as-formed new bands at 1648, 1546, and 1250 cm^{-1} that assigned to amide I, amide II, and amide III vibrational bands, respectively.[33,42] The coating of polymer *P(Thi-diSuc)* on the ITO electrode and chemical reactions between succinimide ends in *P(Thi-diSuc)* and amino ends of anti-PSMA were also investigated with Raman spectroscopy. This technique is the best suitable characterization technique for identifying and understanding biological materials because of important characteristics.[43,44] Of one of them, water doesn't produce significant interference in the Raman spectrum compared to the FTIR technique.[45] Of the other one, sample preparation for Raman spectroscopy is practical and easy.[46] The Raman spectra of *P(Thi-diSuc)* modified and anti-PSMA antibody immobilized ITO electrodes are illustrated in Figures 1C and 1D, respectively. As shown in Figure 1C, the characteristic symmetric and asymmetric carbonyl peaks in succinimide groups were seen at 1772 and 1740 cm^{-1}. The peak at 1813 cm^{-1} was attributed to as-formed new ester bond. In most of studies, the presence of proteins shows three main peaks (amide I, amide II, and amide III). Amide I, amide II, and amide III bond peaks were observed between 1650–1680, 1480–1570, and 1235–1300 cm^{-1}, respectively.[47,48] The peaks of 1651, 1557, and 1336 cm^{-1} were showed as three main peaks in anti-PSMA antibody and were proved to be the presence of antibody on the ITO electrode.

Moreover, the covering of the ITO surface with *P(Thi-diSuc)* polymer was also followed with SEM-EDAX elemental mapping measurement. As seen in, bare ITO had C, O, In, and Sn elements (**Figure 2**A).[34,49] After spin-coating process, it had C, O, S, In, and Sn elements. The observation of S element proved the thiophene ring of *P(Thi-diSuc)* polymer (Figure 2B). Furthermore, to monitor whether a homogenous surface is formed or not, the sulfur element ratios of three areas on the ITO surface were investigated. As monitored in Figure 2, the ratios of Sulphur element were similar, and this similarity proved the homogenous surface coating.

3.1. Electrochemical Characteristics of the Designed ITO Working Electrode

The characteristics of the designed immunosensor fabrication process and PSMA antigen binding on the ITO working electrode were tested EIS and CV techniques. These experiments relating to the electrochemical features of electrodes were taken in 5 mM $[Fe(CN)_6]^{3-/4-}$ 1 M KCl. This redox system as one of the most usually used redox couple in electrochemistry was used to follow the variations generated on the electrode surface. **Figure 3**A,B illustrates the EIS and CV electrochemical behaviors of the biosensor, respectively. Inset of Figure 3A displays the equivalent circuit and it was utilized to fit the EIS data by employing Gamry Echem Analyst software (Table S1A, Supporting Information). This equivalent circuit included electrolyte resistance (R_s), constant phase element (CPE), charge transfer resistance (R_{ct}), and Warburg impedance (W). Nyquist diagram contained a semicircular part and a linear part, which were related to the electron transfer kinetics at higher frequencies and the electron diffusion kinetics at lower frequencies, respectively. The semicircle diameter was equal to the R_{ct}, which was the main element in EIS experiment.[50] As seen in Figure 3A, the R_{ct} value of the *P(Thi-diSuc)* modified electrode was low due to conductivity of the polymer. It provided good electron transfer between electrolyte and electrode surface. After the immobilization of the anti-PSMA antibodies on the ITO surface, the R_{ct} value was

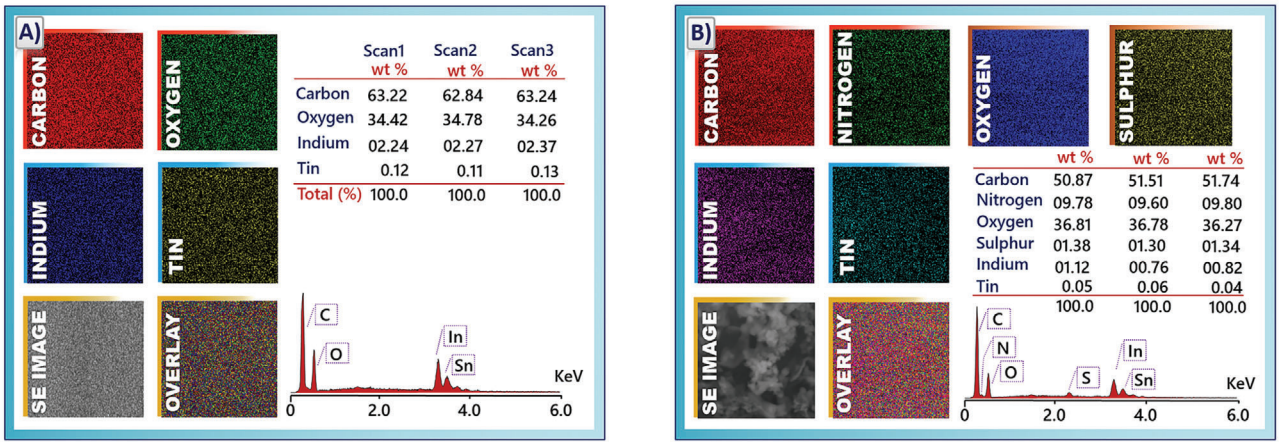

Figure 2. SEM-EDX analyses results of bare ITO and P(Thi-diSuc) covered ITO (A,B).

increased to 3396 Ω. This increase in R_{ct} value mainly originated from nonconductive a protein layer formation, which interfered with the diffusion of electrons to the electrode surface. When the ITO/*P(Thi-diSuc)*/anti-PSMA electrode was treated with BSA, an increased R_{ct} (3631 Ω) value was observed due to the fact that the BSA molecules bound to free active ends of the *P(Thi-diSuc)* polymer present on the ITO surface. At the PSMA antigen step, PSMA antigen immobilization step, PSMA antigens were specifically bound to their antibodies and blocked the electron transfer to the ITO surface. In addition, the electrochemical characteristics of the modified ITO surfaces were investigated utilizing CV technique to support the data obtained from the Nyquist curves. As seen in Figure 3B, pairs of reversible redox peaks (an oxidative and reductive peak) were seen after modifications of ITO electrode. After −0.5 V, the oxidation process started and oxidation increased until it reached to its maximum value. At +0.6 V, the oxidation current reached to maximum value and it was called anodic peak current, ipa and the potential of maximal as anodic peak potential, Epa. The current then decreased as the applied potential surpassed this point. In the reverse cycle, the applied potential swept into the negative direction and the measured current became increasingly negative until it reached the electrochemical reductive potential of the analyte. At −0.3 V, the reduction current reached to maximum value and it was called cathodic peak current, ipc and the potential of maximal as cathodic peak potential, Epc. In addition, at his point, the reduction process reached to diffusion limited. After the anti-PSMA antibodies were bound on the ITO/*P(Thi-diSuc)* surface, the redox peaks were slightly decreased. The immobilization of PSMA specific antibodies prevented the electron transfer and formed a barrier on the electrode surface. The blockage of active ends with BSA created a protein layer formation, which obstructed the electron transfer and decreased the redox peak currents. When the PSMA antigens interacted with anti-PSMA antibodies, the redox peaks were significantly decreased. This decrease displayed that the electron transfer was weakened by immobilization of PSMA antigens on the ITO electrode. These CV findings were consistent with the results of EIS analysis.

3.2. SEM and AFM Studies

The surface morphologies of the different modified bioelectrodes were monitored SEM and AFM analyses. The *P(Thi-diSuc)* polymer layer (**Figure 4**A) was homogenously disrupted on the ITO surface. As observed in AFM image, this polymer modified electrode surface had a high interface area and this surface served as

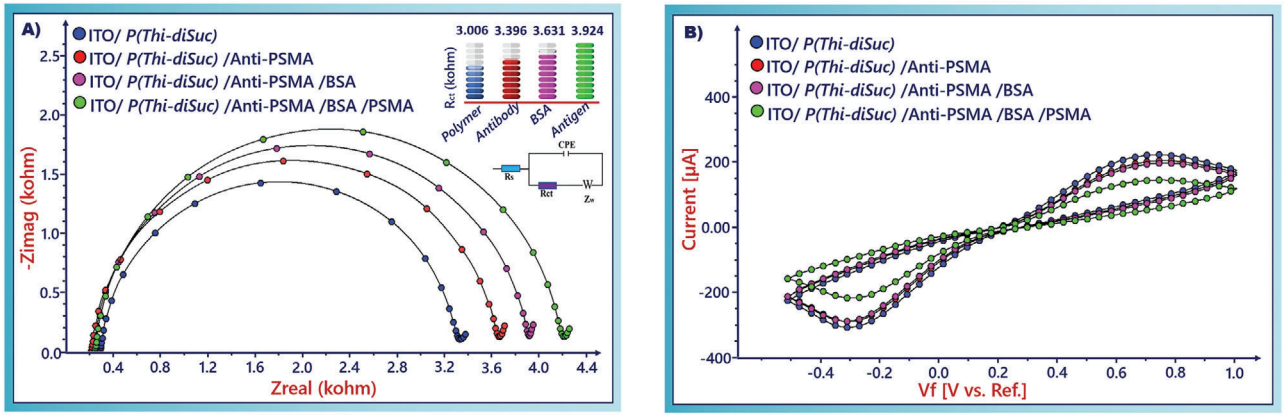

Figure 3. EIS (A) and CVs (B) obtained after each step of immunosensor fabrication. EIS and CV measurements were performed in 5 mM $[Fe(CN)_6]^{3-/4-}$ 1 M KCl.

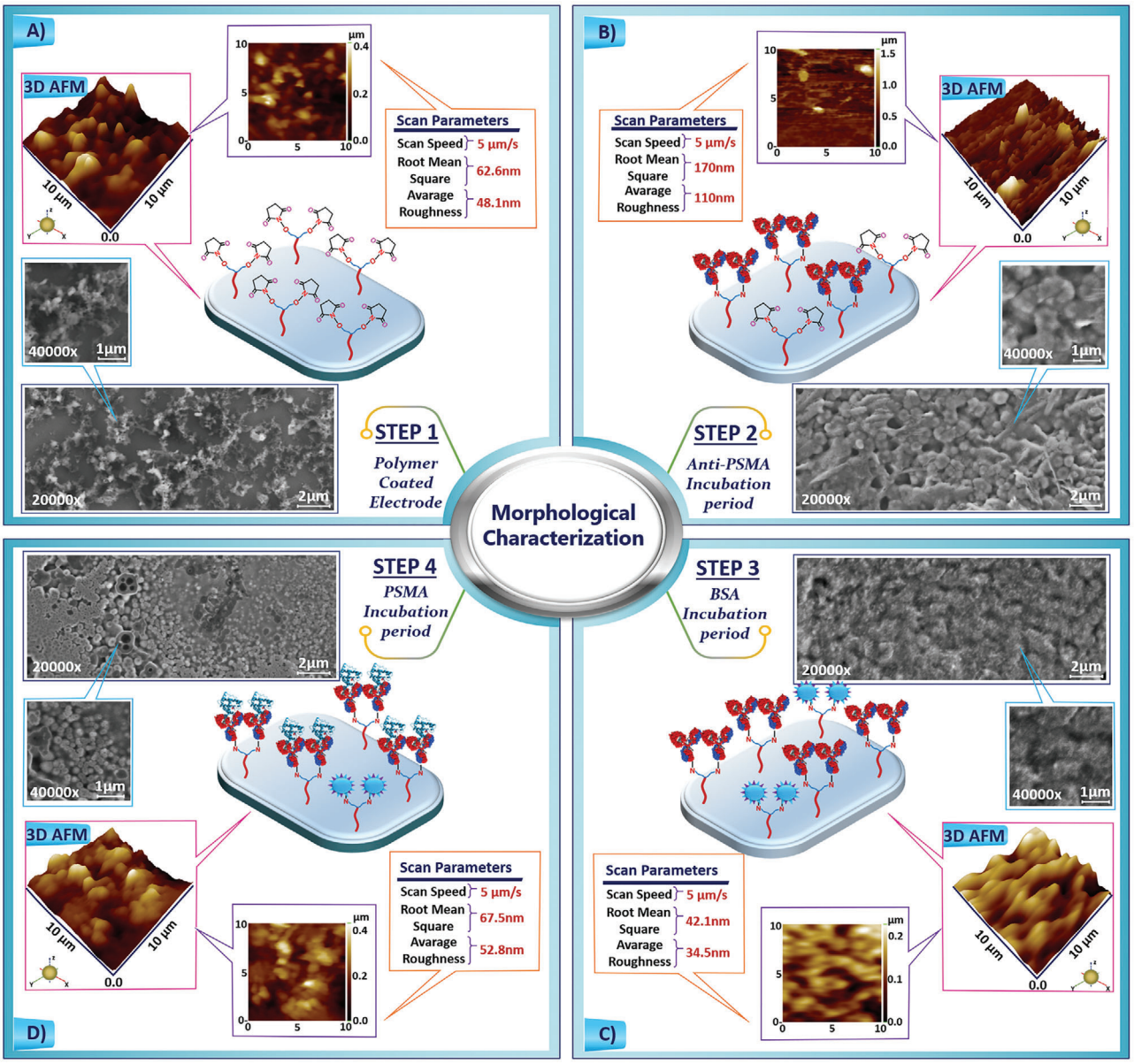

Figure 4. A) SEM and AFM images of polymer coated electrode; B) anti-PSMA antibody, C) BSA and D) PSMA antigen immobilized electrode.

a suitable host for antibodies because it offered more active end sites. The average roughness (R_a) of the *P(Thi-diSuc)* modified surface was 48.1 nm. After covalent linking of anti-PSMA, the working electrode surface morphology was changed and a more globular structure owing to the presence of anti-PSMA antibodies was seen (Figure 4B). The modification step increased the R_a value (110 nm) due to protein layer formation. The BSA blockage process varied the sensor surface morphology and a smooth surface was obtained. After coupling free ends with BSA molecule, the R_a was measured as 34.5 nm (Figure 4C). The covalent immobilization of PSMA antigens on the prepared ITO/*P(Thi-diSuc)*/anti-PSMA/BSA surface changed the electrode surface morphology and PSMA antigen molecules were clearly seen on the ITO platform. The specific immuno-interaction between anti-PSMA and PSMA antigen raised the R_a and it was found as 52.8 nm (Figure 4D).

3.3. Optimum Experimental Parameters Selection for Biosensor Fabrication

To optimize the experimental parameters for the successful determination of PSMA antigen, several experiments were carried out. First of all, the amount of polymer, which was used for immobilization of biomolecules, was optimized. Three different polymer amounts were utilized and the variation in R_{ct} from the signals of the EIS analysis depending on the different polymer amounts (0.13, 0.26, and 0.39 mg mL^{-1}) was plotted. A low

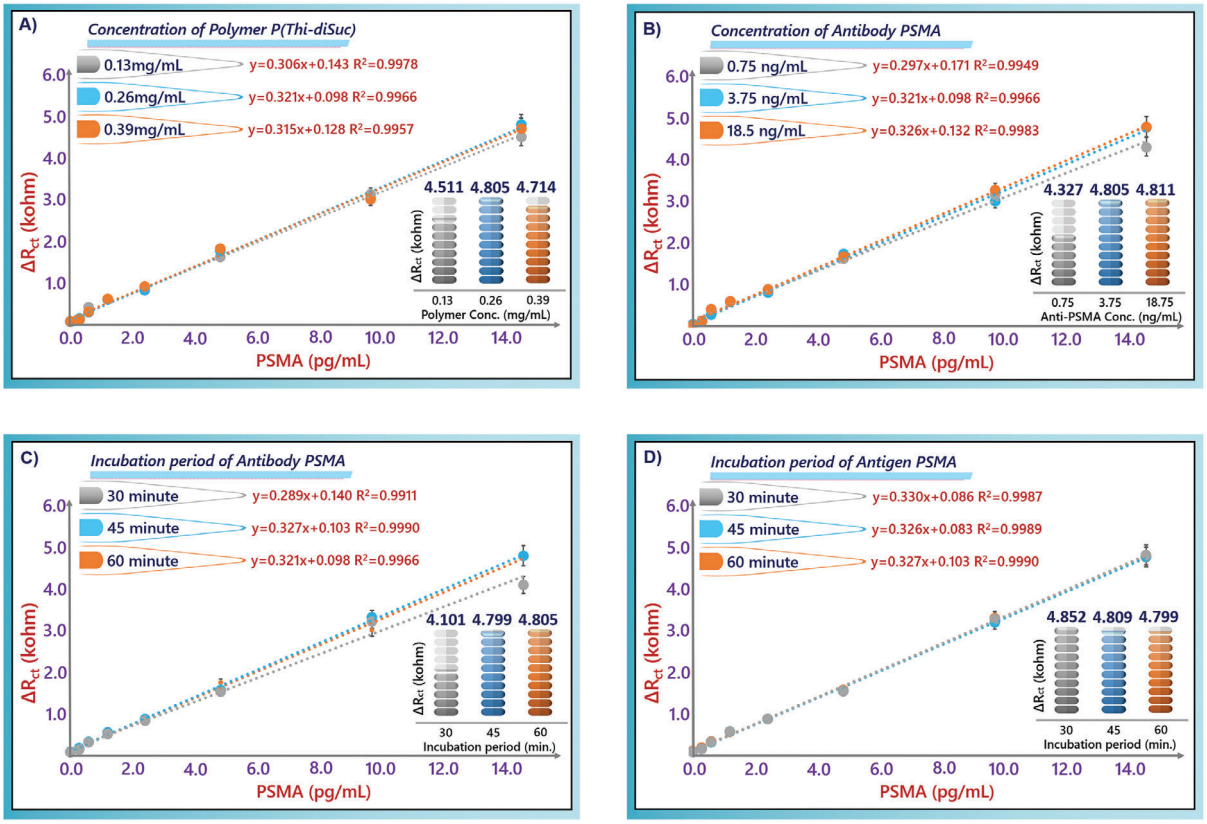

Figure 5. Optimization graphs for effect of polymer amount (A), anti-PSMA amount (B), anti-PSMA immobilization time (C), and PSMA immobilization time (D).

amount of polymer (0.13 mg mL^{-1}) provided a low immunosensor signal and the increment in polymer amount increased the immunosensor signal. The signals of immunosensors fabricated using 0.26 and 0.39 mg mL^{-1} polymer amounts were similar and therefore, 0.26 mg mL^{-1} polymer amount was chosen as an optimum value (**Figure 5**A). The amount of biorecognition molecule, which provided specific detection of PSMA antigen is another important point. To create the required surface for specific biointeraction between antibody and antigen, three different anti-PSMA antibody amounts were utilized (0.75, 3.75, and 18.75 ng mL^{-1}). The variation in R_{ct} signals from the results of EIS analysis depending on the different biorecognition element concentrations was plotted. The increment in the utilized antibody amount increased the immunosensor signal and then, it was stabilized. Therefore, 3.75 ng mL^{-1} was selected optimum biorecognition element amount (Figure 5B). The effect of anti-PSMA antibody incubation period on the immunosensor signal was investigated. The prepared ITO/*P(Thi-diSuc)* electrodes were incubated in anti-PSMA solution for three different durations (30, 45, and 60 min). The variation in R_{ct} from the signals of EIS analysis depending on the different incubation durations was plotted. The R_{ct} increased as the incubation time increased. The signals after 45 min-incubation and 60 min-incubation were close to each other and the R_{ct} value no longer increased. Thanks to the fact that 45 min was used as optimal incubation duration (Figure 5C). In addition, the effect of antigen incubation period was also studied. For this experiment, three different times (30, 45, and 60 min) were utilized. As monitored in Figure 5D, the immunosensor signals were close to each other after three different incubation times and 30 min was enough for binding between antibody and antigen.

3.4. Ultrasensitive Determination of PSMA Antigen Using the Proposed Immunosensor

Under the optimum experimental parameters, the electrochemical behavior of the biosensor to PSMA antigen was recorded in 5 mM $[Fe(CN)^6]^{3-/4-}$ including 1 M KCl. As seen in **Figure 6**A, the semicircle diameter of Nyquist plot after PSMA antigen immobilization, at different concentrations of PSMA increased proportionally with the increment in PSMA antigen amount in the detection range of (0.015 to 14.4 pg mL^{-1}). For the reason of the insulating features of PSMA antigen, the R_{ct} was increased from 3747 to 8475 Ω (Table S1B, Supporting Information). At the same time, because of the same reason, the peak currents of CV were decreased with the increment in PSMA antigen amount (Figure 6C). These circumstances proved the low electron transfer rate formation after PSMA antigen molecules immobilization. Figure 6B displays the linear dependence between the ΔR_{ct} and PSMA antigen level in the range of 0.015–14.4 pgmL^{-1} with a limit of detection (LOD) of 4.7 fgmL^{-1} (signal-to-noise ratio of 3σ, σ is the standard deviation of blank sample, $n = 3$). The regression equation, correlation coefficient, and sensitivity were

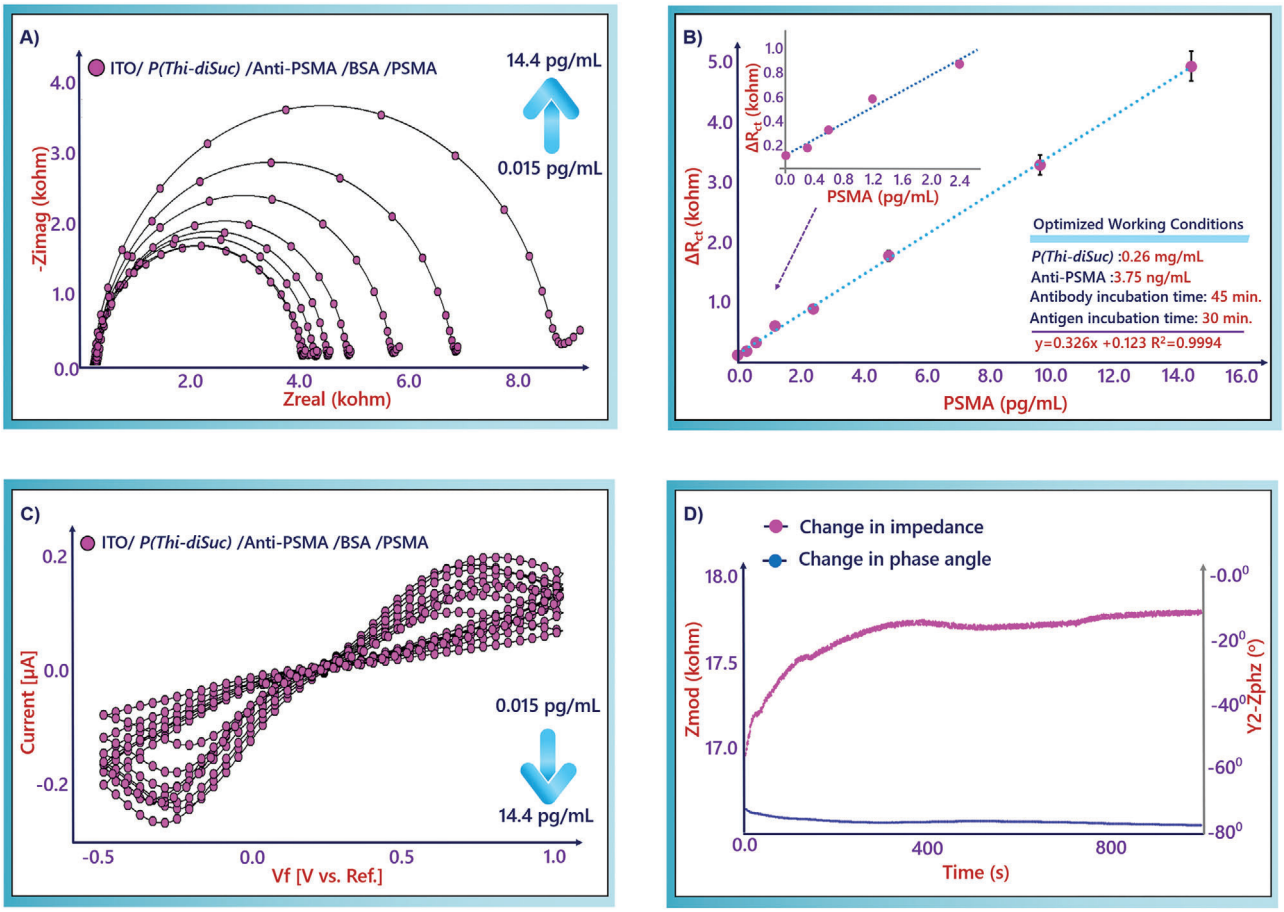

Figure 6. Nyquist plots (A) and CVs (C) of the proposed immunosensor treated by different levels of PSMA. Calibration curve for impedimetric PSMA immunosensor (B). SFI analysis result (D).

found as $\Delta R_{ct} = 0.327$ [PSMA]+0.124, $R^2 = 0.9994$ and 1.36 $k\Omega pg^{-1}mLcm^{-2}$, respectively. The detection performance of the prepared biosensor was compared with to PSMA analysis methods. A comparison with other techniques for the analysis of PSMA is shown in **Table 1**A. As displayed in Table 1A, our biosensor had a lower limit of detection (LOD) than other methods. Furthermore, this immunosensor was an easy and cost-efficient way for PSMA detection.

Single frequency impedance is a successful technique for examination of specific biointeraction between antibody and antigen. This technique is applied at a single frequency and utilized for impedance measurement versus time during the changes.[51] In this biosensing system, a single frequency (13 Hz), which was acquired from Bode diagram was utilized and used for monitoring of specific immuno-interaction between anti-PSMA and PSMA antigen. As observed in Figure 6D, the increment in impedance confirmed the specific immuno-interaction.

3.5. Repeatability, Reproducibility, Storage-Stability, and Reusability of the Impedance Biosensor

Under optimum conditions, the repeatability and reproducibility of the proposed biosensor were tested. In order to test the repeatability of the biosensor, 20 electrodes were independently prepared, and treated to 2.4 pg mL^{-1} PSMA antigen. Relative standard deviation (RSD) of the impedimetric signals for determination of PSMA antigen was 2.39%. The result illustrated that this biosensor had acceptable repeatability (**Figure 7**A). In order to normality of the repeatability test results, Shapiro–Wilk test was performed. This test is a powerful test for normality determination. The Shapiro–Wilk test examines the normally distributed property of a variable in a population. The test rejects the hypothesis of normality when p-value is less than or equal to 0.05.[52] By using Shapiro–Wilk test, the p-value of this study was found as 0.492 and because of this result (0.492 > 0.05) our test result illustrated normally distributed.

Skewness is a degree of asymmetry of distribution. It measures the lack of symmetry in data distribution. Perfectly symmetrical distribution has a skewness equal to zero. Positive skewness means when the tail on the right side of the distribution is longer. Negative skewness means when the tail on the left side of the distribution is longer than the right side. The skewness of the repeatability data set was found as 0.393 and this value illustrated the fairly symmetrical of distribution.[53] Kurtosis is a degree of peakedness of data distribution. The positive kurtosis shows the distribution whose data values are more concentrated around the mean than in a normal

Table 1. Comparison of the suggested immunosensor with other techniques for the detection of PSMA antigen (A). The detection results and recovery study results of the proposed immunosensor (B).

(A)

Methods	Applied materials	Detection range [pg mL^{-1}]	Detection limit [pg mL^{-1}]	Reference
Radioenzymatic assay	*N*-acetyl-L-aspartyl-L-glutamate	1300–17 200	–	[58]
Magnetically assisted surface enhanced Raman spectroscopy	Fe3O4@Ag magnetic nanocomposite	5000–2×10^5	480	[2]
Love wave sensor	Molecularly imprinted polymer	10–10^5	13	[9]
Electrochemical	Phage-PEDOT film modified gold	–	10^5	[14]
Optical	Parallel optical read-out of micromechanical pillars	30×10^3–10^7	3×10^4	[24]
Electrochemical	M13 virus-PEDOT modified glass	2×10^3–12×10^3	5600	[13]
Electrochemical	*P(Thi-diSuc)* modified ITO	0.015–14.4	0.0064	This study
ELISA kit	Quantitative sandwich	469–3×10^4	281	MyBioSource
ELISA kit	Quantitative sandwich	469–3×10^4	281	Elabscience
ELISA kit	Quantitative sandwich	469–3×10^4	281	LsBio

(B)

Sample	Measured by biosensor [pg mL^{-1}]	Added PSMA antigen [pg mL^{-1}]	*SD and *CV [%]	Total measured by biosensor	*SD and *CV [%]	Recovery [%]	Relative difference [%]
1	1.24	1	0.03, 2.75	2.38	0.02, 0.81	106.30	6.30
1	1.29	1		2.40		105.23	5.23
2	3.67	1	0.04, 1.17	4.95	0.20, 4.23	105.90	5.90
2	3.73	1		4.66		98.45	−1.55
3	2.90	1	0.06, 2.06	3.92	0.18, 4.53	100.71	0.71
3	2.98	1		4.18		105.07	5.07
4	3.68	1	0.18, 4.66	4.69	0.28, 5.71	100.13	0.13
4	3.93	1		5.08		103.04	3.04
5	1.42	1	0.06, 4.01	2.48	0.03, 1.21	102.54	2.54
5	1.50	1		2.52		100.86	0.86

*SD: Standard Deviation, *CV: Coefficient Variation.

distribution. The negative kurtosis illustrates the distribution which is more dispersed than in a normal distribution. The kurtosis of the repeatability data set was found as −0.314 and this value illustrated the platykurtic distribution.[54]

Grubbs's test detects outliers from normal distributions. This test is operated using the mean and standard deviation of the data. The Grubbs's test value is compared with the fixed value (level of significance) present in the table. According to null hypothesis, the suspected value as an outlier is accepted if the Grubbs's test value is smaller than the fixed value. When the Grubbs's test was applied to our repeatability data set, the Grubbs's test values (1.396 (low) and 2.223 (high)) were lower than tabulated value at $\alpha = 0.05$ (2.709).[55] Apart from Grubbs's test, in order to determine the outliers, Dixon's Q test was also performed. The Dixon's test values of repeatability data set were found as 0.020 (low outlier) and 0.242 (high outlier) and these valves were lower than the tabulated critical value 0.477 ($\alpha = 0.05$).[56]

To test reproducibility, ten different biosensors were prepared and used for PSMA detection. As seen in Figure 7B, the calibration plots of these biosensors were overlapped and also, they produced reproducible signals. Horwitz ratio illustrates the acceptability of analysis methods with respect to reproducibility test. In order to calculate Horwitz ratio, relative standard deviation (RSD_R (%)) and predicted relative deviation calculated from the Horwitz equation ($PRDS_R(\%) = 2C^{-0.15}$) is utilized. The low ratio (<0.5) illustrates the excellent training and experience, and the high ratio (>2) shows inhomogeneity of test samples and requirement of method optimization and training.[57] In this reproducibility study, the Horwitz ratios of each concentration level were ranged from 0.08–0.70 and these low ratios proved the acceptability of the study.

Moreover, to prove the storage-stability of the biosensor, the prepared ITO/*P(Thi-diSuc)*/anti-PSMA/BSA electrodes were stored at 4 °C. After incubation in PSMA antigen solution (2.4 pg mL^{-1}), the immunosensor signal was measured in each week and it had 92.84% of the initial signal after 8 weeks (Figure 7C). The obtained results displayed that polymer modified ITO electrode maintained high stability over a long period for PSMA antigen detection.

To examine the reusability of the biosensor, the produced ITO/*P(Thi-diSuc)*/anti-PSMA/BSA/PSMA electrode was immersed in acidic solution (0.1% HCl) for 5 min. After rinsing with ultrapure water, it was utilized again for PSMA (2.4 pg mL^{-1})

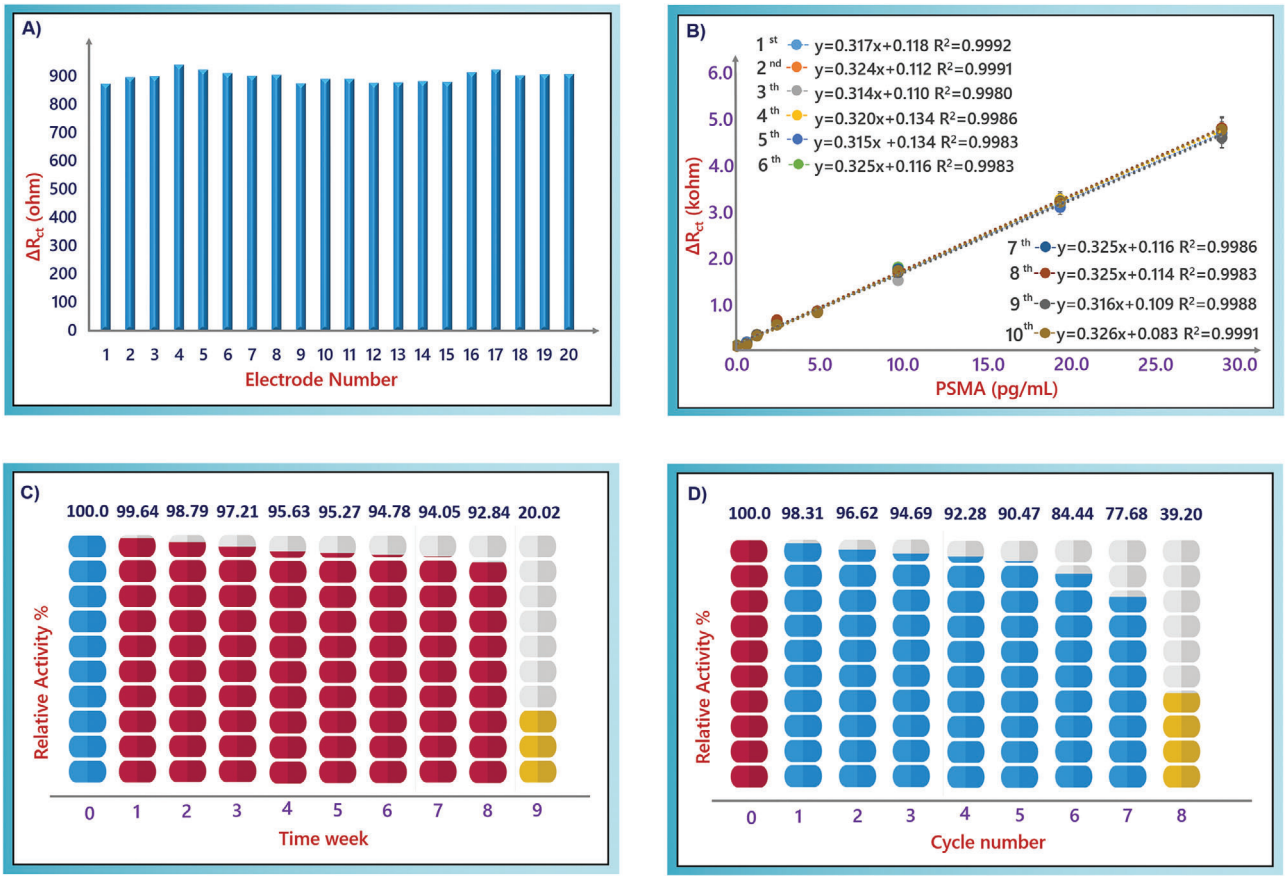

Figure 7. Repeatability (A), reproducibility (B), storage-stability (C), and regeneration (D) results of the proposed biosensor.

analysis. As displayed in Figure 7D, the immunosensor illustrated reusability till 7th regeneration cycle retaining 77.68% of impedimetric signal. This result suggested that the immunosensor was suitable for multiple PSMA measurement.

In order to evaluate the selectivity of the suggested sensor, the electrochemical behaviors of ITO/*P(Thi-diSuc)*/anti-PSMA/BSA electrode was tested by incubation in PBS solution containing interference proteins. The change of electrochemical signal according to the presence and absence of the interference proteins (interleukin 6, kallikrein 4, interleukin 1α, and interleukin 8 with 240 pg mL^{-1} concentration) illustrated in Figure S5, Supporting Information. In the absence of PSMA antigen, a low signal was obtained. In contrast to this result, the immunosensor gave a high signal to PSMA antigen (2.4 pg mL^{-1}). From these results, the suggested immunosensor could selectively detect PSMA antigen in the presence of interference proteins.

3.6. PSMA Determination in Serum Samples

In order to test whether this suggested immunosensing platform could be used in the analysis of real samples, human serums were chosen as real samples. Before the analyses, these serum samples were diluted 1000-fold. After dilution, PSMA antigen spiked to these samples to examine the accuracy of the proposed biosensor. As seen in Table 1B, the developed immunosensor exhibited good recovery rates (98.45–106.30%) and it was a suitable tool for PSMA detection. The obtained high recovery rates proved the feasibility of the immunosensor for real application in human serum.

4. Conclusion

In the current study, a sensitive, stable, and label-free biosensor based on covalent binding of anti-PSMA antibodies onto disuccinimide substituted polythiophene polymer coated ITO substrate was developed for the direct assay of PSMA antigen. This *P(Thi-diSuc)* polymer was synthesized to shorten the fabrication process. Because, it had succinimide side groups and these active groups directly linked to the antibodies. The suggested immunosensor was characterized by using CV and EIS in the presence of $[Fe(CN)_6]^{3-}/[Fe(CN)_6]^{4-}$ redox couple. Before employing the biosensor for testing, a number of main conditions such as amount of anti-PSMA and polymer, and the incubation duration of anti-PSMA and PSMA were optimized. Because of the good conductivity and biocompatibility of *P(Thi-diSuc)* polymer, the designed immunosensor had a wide linear detection range of 0.015–14.4 pgmL^{-1}, a good repeatability, and an excellent reproducibility. The detection limit of the proposed biosensor was found to be 6.4 fgmL^{-1}, which was lower than other techniques. The selectivity of the fabricated biosensor was tested against other cancer biomarkers. Furthermore, the suggested immunosensor

($0.07 per test) was able to analyze the PSMA antigen level much cheaper than ELISA test ($5.10 per test). The suggested biosensor was interesting and with a user-friendly aspect to determine PSMA serum concentrations and it was more proper than ELISA kit. Finally, the biosensor was validated for the quantification of PSMA in real human serum and it exhibited high recovery rates (98.45–106.30%). In conclusion, this novel immunosensor would have widespread applications in the detection of biomarkers in the future.

Supporting Information

Supporting Information is available from the Wiley Online Library or from the author.

Acknowledgements

The authors would like to acknowledge the financial support from The Scientific and Technological Research Council of Tekirdağ Namık Kemal University, NKU-BAP (NKUBAP.00.ÖNAP.19.209).

Conflict of Interest

The authors declare no conflict of interest.

Data Availability Statement

Data available on request from the authors.

Keywords

di-succinimide substituted polythiophene polymer, electrochemical impedance spectroscopy, indium tin oxide, prostate specific membrane antigen

Received: April 24, 2021
Revised: June 26, 2021
Published online:

[1] M. A. Najeeb, Z. Ahmad, R. A. Shakoor, A. M. A. Mohamed, R. Kahraman, *Talanta* **2017**, *168*, 52.
[2] Z. Chaloupková, A. Balzerová, J. Bařinková, Z. Medříková, P. Šácha, P. Beneš, V. Ranc, J. Konvalinka, R. Zbořil, *Anal. Chim. Acta* **2018**, *997*, 44.
[3] E. B. Aydın, M. Aydın, M. K. Sezgintürk, *Sens. Actuators, B* **2020**, *325*, 128788.
[4] K. Zhang, S. Lv, Z. Lin, D. Tang, *Biosens. Bioelectron.* **2017**, *95*, 34.
[5] J. Chen, F. Xue, Z. Yu, L. Huang, D. Tang, *Analyst* **2020**, *145*, 7186.
[6] G. Cai, Z. Yu, P. Tong, D. Tang, *Nanoscale* **2019**, *11*, 15659.
[7] S. Lv, K. Zhang, D. Tang, *Analyst* **2019**, *144*, 3716.
[8] S. Lv, Z. Lin, K. Zhang, M. Lu, D. Tang, *Anal. Chim. Acta* **2017**, *964*, 67.
[9] P. Tang, Y. Wang, J. Huo, X. Lin, *Polymers* **2018**, *10*, 563.
[10] E. B. Aydın, M. Aydın, M. K. Sezgintürk, *Talanta* **2021**, *222*, 121596.
[11] M. Inubushi, T. Kaneta, T. Ishimori, E. Imabayashi, A. Okizaki, N. Oku, *Ann. Nucl. Med.* **2017**, *31*, 571.
[12] R. Seenivasan, C. K. Singh, J. W. Warrick, N. Ahmad, S. Gunasekaran, *Biosens. Bioelectron.* **2017**, *95*, 160.
[13] J. A. Arter, J. E. Diaz, K. C. Donavan, T. Yuan, R. M. Penner, G. A. Weiss, *Anal. Chem.* **2012**, *84*, 2776.
[14] K. Mohan, K. C. Donavan, J. A. Arter, R. M. Penner, G. A. Weiss, *J. Am. Chem. Soc.* **2013**, *135*, 7761.
[15] P. Mhawech-Fauceglia, S. Zhang, L. Terracciano, G. Sauter, A. Chadhuri, F. R. Herrmann, R. Penetrante, *Histopathology* **2007**, *50*, 472.
[16] Y. H. Park, H. W. Shin, A. R. Jung, O. S. Kwon, Y.-J. Choi, J. Park, J. Y. Lee, *Sci. Rep.* **2016**, *6*, 30386.
[17] S. Lv, K. Zhang, Y. Zeng, D. Tang, *Anal. Chem.* **2018**, *90*, 7086.
[18] K. Zhang, S. Lv, Z. Lin, M. Li, D. Tang, *Biosens. Bioelectron.* **2018**, *101*, 159.
[19] Q. Zhou, Y. Lin, K. Zhang, M. Li, D. Tang, *Biosens. Bioelectron.* **2018**, *101*, 146.
[20] G. Cai, Z. Yu, R. Ren, D. Tang, *ACS Sens.* **2018**, *3*, 632.
[21] E. B. Aydın, M. Aydın, M. K. Sezgintürk, *Talanta* **2020**, *222*, 121596.
[22] D. Grieshaber, R. Mackenzie, J. Vörös, E. Reimhult, *Sensors* **2008**, *8*, 1400.
[23] A. Juzgado, A. Soldà, A. Ostric, A. Criado, G. Valenti, S. Rapino, G. Conti, G. Fracasso, F. Paolucci, M. Prato, *J. Mater. Chem. B* **2017**, *5*, 6681.
[24] M. Tardivo, V. Toffoli, G. Fracasso, D. Borin, S. Dal Zilio, A. Colusso, S. Carrato, G. Scoles, M. Meneghetti, M. Colombatti, M. Lazzarino, *Biosens. Bioelectron.* **2015**, *72*, 393.
[25] M. Xu, Z. Gao, Q. Wei, G. Chen, D. Tang, *Biosens. Bioelectron.* **2015**, *74*, 1.
[26] L. Hou, Y. Tang, M. Xu, Z. Gao, D. Tang, *Anal. Chem.* **2014**, *86*, 8352.
[27] L. Hou, X. Wu, G. Chen, H. Yang, M. Lu, D. Tang, *Biosens. Bioelectron.* **2015**, *68*, 487.
[28] Z. Qiu, D. Tang, J. Shu, G. Chen, D. Tang, *Biosens. Bioelectron.* **2016**, *75*, 108.
[29] R. Ohno, H. Ohnuki, H. Wang, T. Yokoyama, H. Endo, D. Tsuya, M. Izumi, *Biosens. Bioelectron.* **2013**, *40*, 422.
[30] E. B. Aydın, M. Aydın, M. K. Sezgintürk, *Biosens. Bioelectron.* **2017**, *97*, 169.
[31] M. Aydın, E. B. Aydın, M. K. Sezgintürk, *Biosens. Bioelectron.* **2018**, *117*, 720.
[32] M. Akgün, M. Kemal Sezgintürk, *Int. J. Environ. Anal. Chem.* **2020**, *100*, 432.
[33] E. B. Aydın, M. Aydın, M. K. Sezgintürk, *Sens. Actuators, B* **2020**, *306*, 127613.
[34] M. Aydın, E. B. Aydın, M. K. Sezgintürk, *Biosens. Bioelectron.* **2019**, *126*, 230.
[35] T. K. Das, S. Prusty, *Polym.-Plast. Technol. Eng.* **2012**, *51*, 1487.
[36] A. Ramanavičius, A. Ramanavičienė, A. Malinauskas, *Electrochim. Acta* **2006**, *51*, 6025.
[37] D. Odaci, S. Kiralp Kayahan, S. Timur, L. Toppare, *Electrochim. Acta* **2008**, *53*, 4104.
[38] L. Kumpumbu-Kalemba, M. Leclerc, *Chem. Commun.* **2000**, 1847.
[39] D. Thanasamy, D. Jesuraj, S. K. Konda Kannan, V. Avadhanam, *Polymer* **2019**, *175*, 32.
[40] B. Dordi, J. P. Pickering, H. Schönherr, G. J. Vancso, *Surf. Sci.* **2004**, *570*, 57.
[41] C. Y. Lim, N. A. Owens, R. D. Wampler, Y. Ying, J. H. Granger, M. D. Porter, M. Takahashi, K. Shimazu, *Langmuir* **2014**, *30*, 12868.
[42] M. Khanmohammadi, A. B. Garmarudi, *TrAC, Trends Anal. Chem.* **2011**, *30*, 864.
[43] S. Rangan, H. G. Schulze, M. Z. Vardaki, M. W. Blades, J. M. Piret, R. F. B. Turner, *Analyst* **2020**, *145*, 2070.
[44] L. A. Austin, S. Osseiran, C. L. Evans, *Analyst* **2016**, *141*, 476.
[45] H. J. Byrne, P. Knief, M. E. Keating, F. Bonnier, *Chem. Soc. Rev.* **2016**, *45*, 1865.

[46] I. Pence, A. Mahadevan-Jansen, *Chem. Soc. Rev.* **2016**, *45*, 1958.
[47] M. Miletić, S. Aškrabić, J. Rüger, B. Vasić, L. Korićanac, A. S. Mondol, J. Dellith, J. Popp, I. W. Schie, Z. Dohčević-Mitrović, *Analyst* **2020**, *145*, 3983.
[48] I. H. Boyaci, H. T. Temiz, H. E. Geniş, E. Acar Soykut, N. N. Yazgan, B. Güven, R. S. Uysal, A. G. Bozkurt, K. İlaslan, O. Torun, F. C. Dudak Şeker, *RSC Adv.* **2015**, *5*, 56606.
[49] E. B. Aydın, M. Aydın, A. Yuzer, M. Ince, K. Ocakoğlu, M. K. Sezgintürk, *ACS Biomater. Sci. Eng.* **2021**, *7*, 1192.
[50] J. Park, W. Lee, I. Kim, M. Kim, S. Jo, W. Kim, H. Park, G. Lee, W. Choi, D. S. Yoon, J. Park, *Sens. Actuators, B* **2019**, *293*, 296.
[51] E. B. Aydın, M. Aydın, M. K. Sezgintürk, *New J. Chem.* **2020**, *44*, 14228.
[52] J. P. Royston, *J. R. Stat. Soc.: Ser. C (Appl. Stat.)* **1983**, *32*, 121.
[53] G. Békés, G. Kézdi, *Data Analysis for Business, Economics, and Policy*, Cambridge University Press, Cambridge **2021**, p. 144.
[54] R. Kitchin, N. Thrift, *International Encyclopedia of Human Geography*, Elsevier, New York **2009**.
[55] M. Aslam, *J. King Saud Univ.-Sci.* **2020**, *32*, 2696.
[56] S. Walfish, *Pharm. Technol.* **2006**, *30*, 82.
[57] W. Horwitz, R. Albert, *J. AOAC Int.* **2006**, *89*, 1095.
[58] T. Knedlík, V. Navrátil, V. Vik, D. Pacík, P. Šácha, J. Konvalinka, *Prostate* **2014**, *74*, 768.